SAND2014-4837C

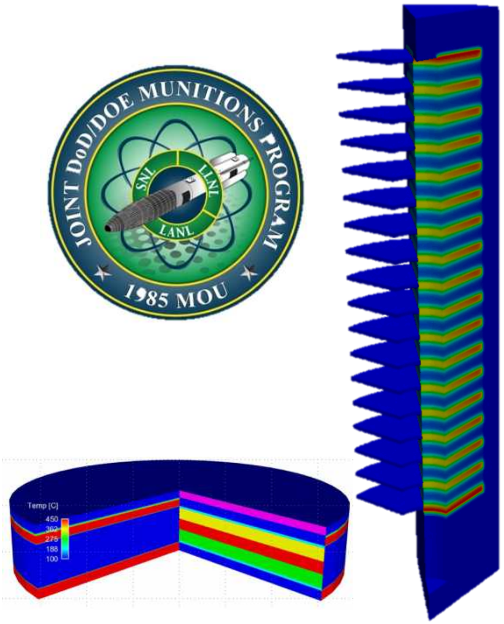

Towards a Coupled Multiphysics Model of Molten Salt Battery Mechanics

Scott A. Roberts, Kevin N. Long, Jonathan R. Clausen, Mario J. Martinez, Edward S. Piekos, and Anne M. Grillet

Engineering Sciences Center
Sandia National Laboratories, Albuquerque, NM
sarober@sandia.gov

Session 28: Molten Salt Batteries (Primary & Secondary) II, 46th Power Sources Conference, Orlando, FL

June 11, 2014

Sandia National Laboratories

Exceptional service in the national interest

U.S. DEPARTMENT OF ENERGY

NNSA National Nuclear Security Administration

Sandia National Laboratories is a multi-program laboratory managed and operated by Sandia Corporation, a wholly owned subsidiary of Lockheed Martin Corporation, for the U.S. Department of Energy's National Nuclear Security Administration under contract DE-AC04-94AL85000.

Physical mechanisms in molten salt battery activation

- Battery activation is a complicated, multi-step process
  - Heat pellet burning
  - Thermal diffusion
  - Melting of the electrolyte
  - Deformation of the separator
  - Flow of the electrolyte
  - Activation

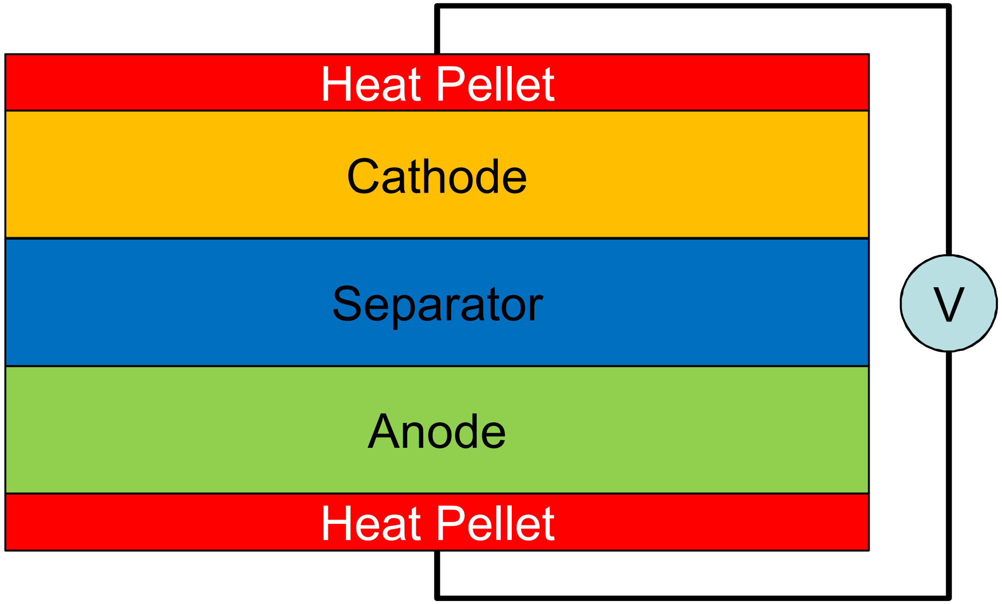

- A true multi-physics problem
  - Thermal
  - Mechanical
  - Fluid
  - Electrochemical
- Why performance models of thermal batteries?
  - Predict activation times
  - Optimize volume, insulation, manufacturing

Physical mechanisms in molten salt battery activation

- Battery activation is a complicated, multi-step process
  - Heat pellet burning
  - Thermal diffusion
  - Melting of the electrolyte
  - Deformation of the separator
  - Flow of the electrolyte
  - Activation

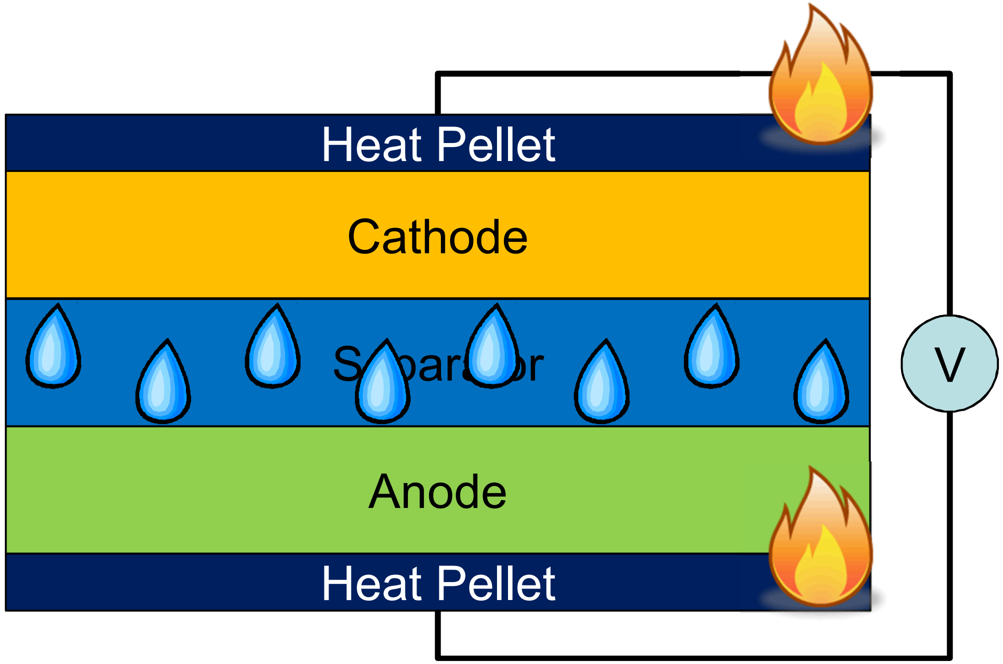

- A true multi-physics problem
  - Thermal
  - Mechanical
  - Fluid
  - Electrochemical

- Why performance models of thermal batteries?
  - Predict activation times
  - Optimize volume, insulation, manufacturing

Physical models and couplings: Current

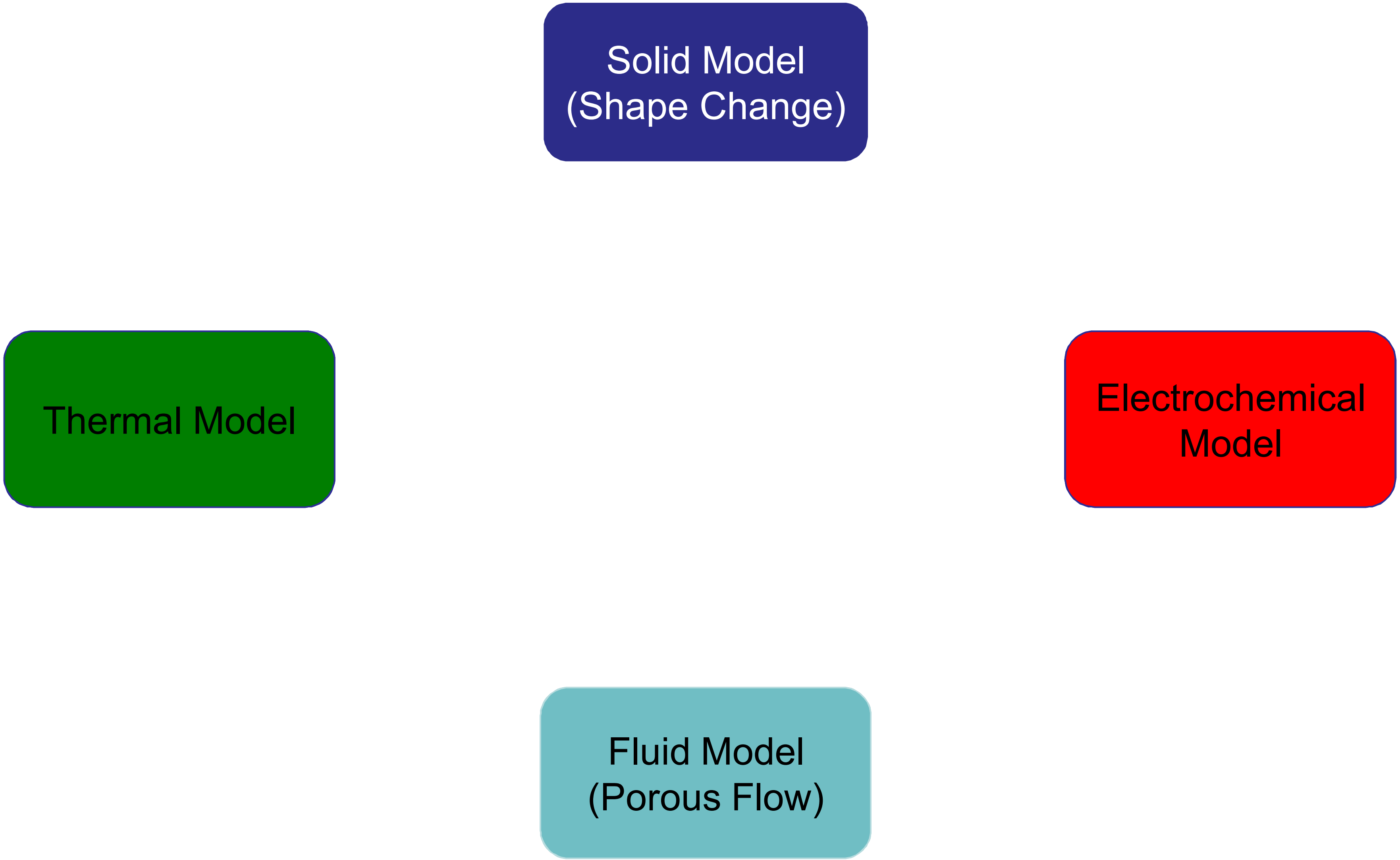

Physical models and couplings: Current

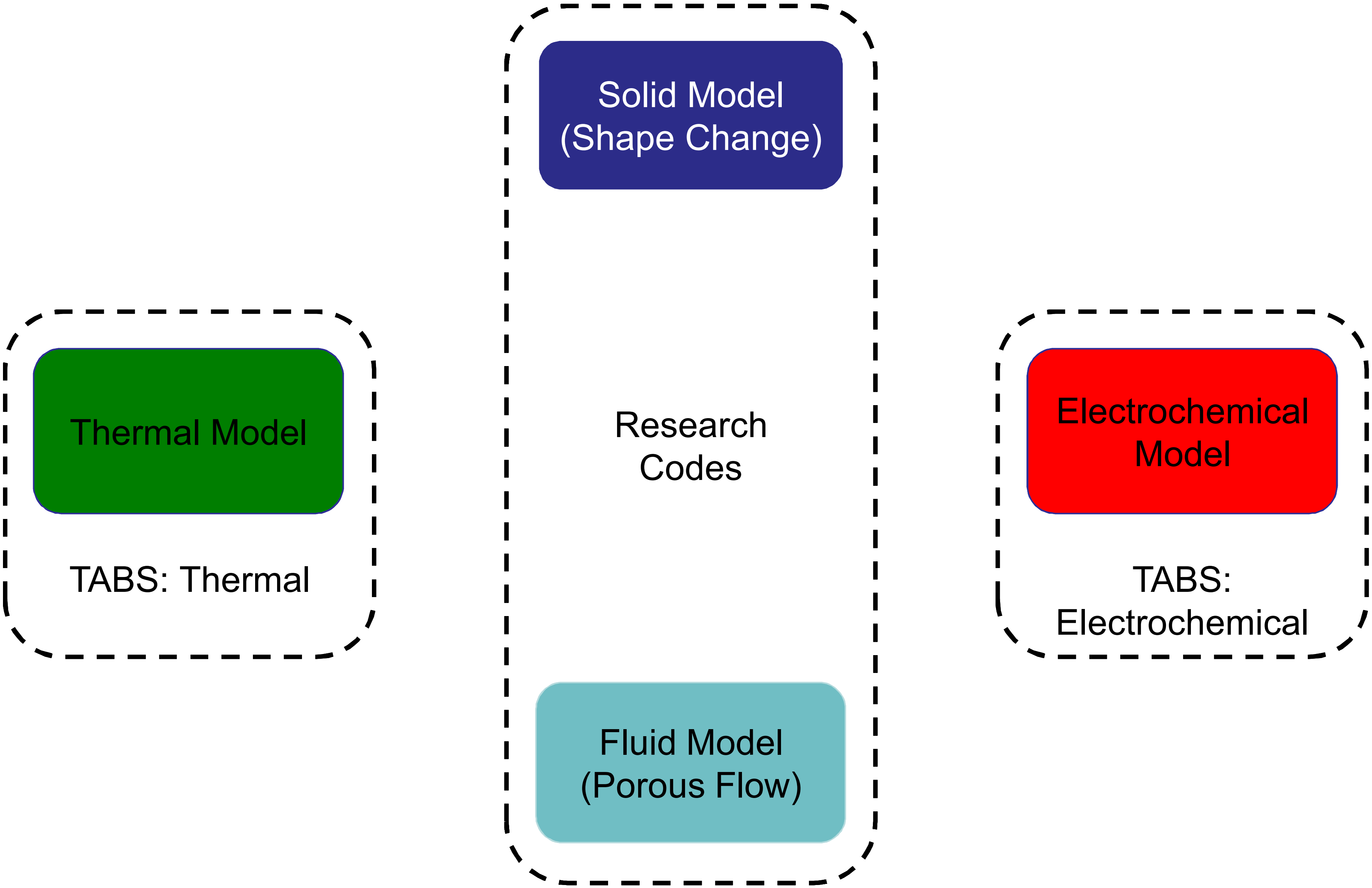

Physical models and couplings: Obvious

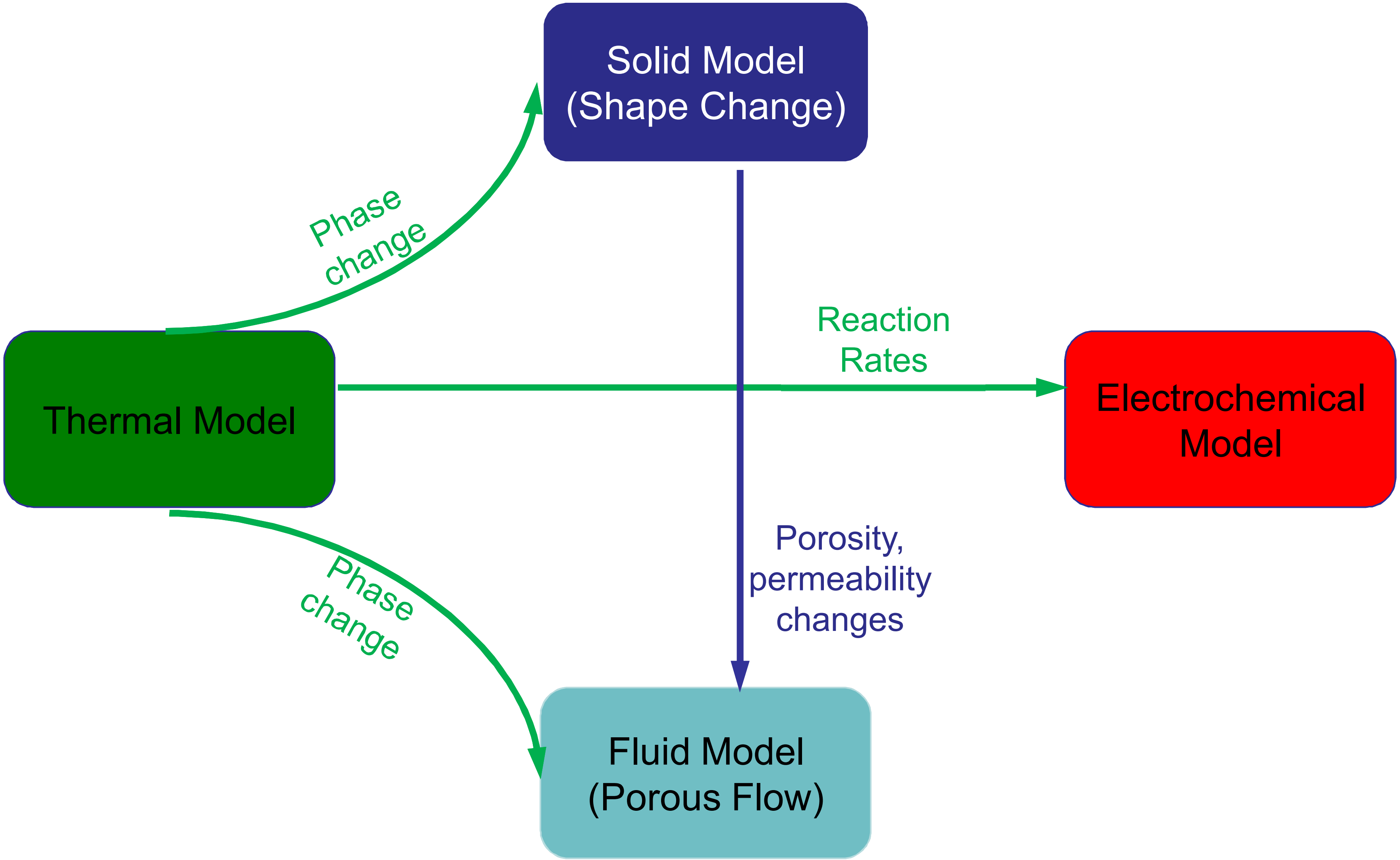

Physical models and couplings: Everything

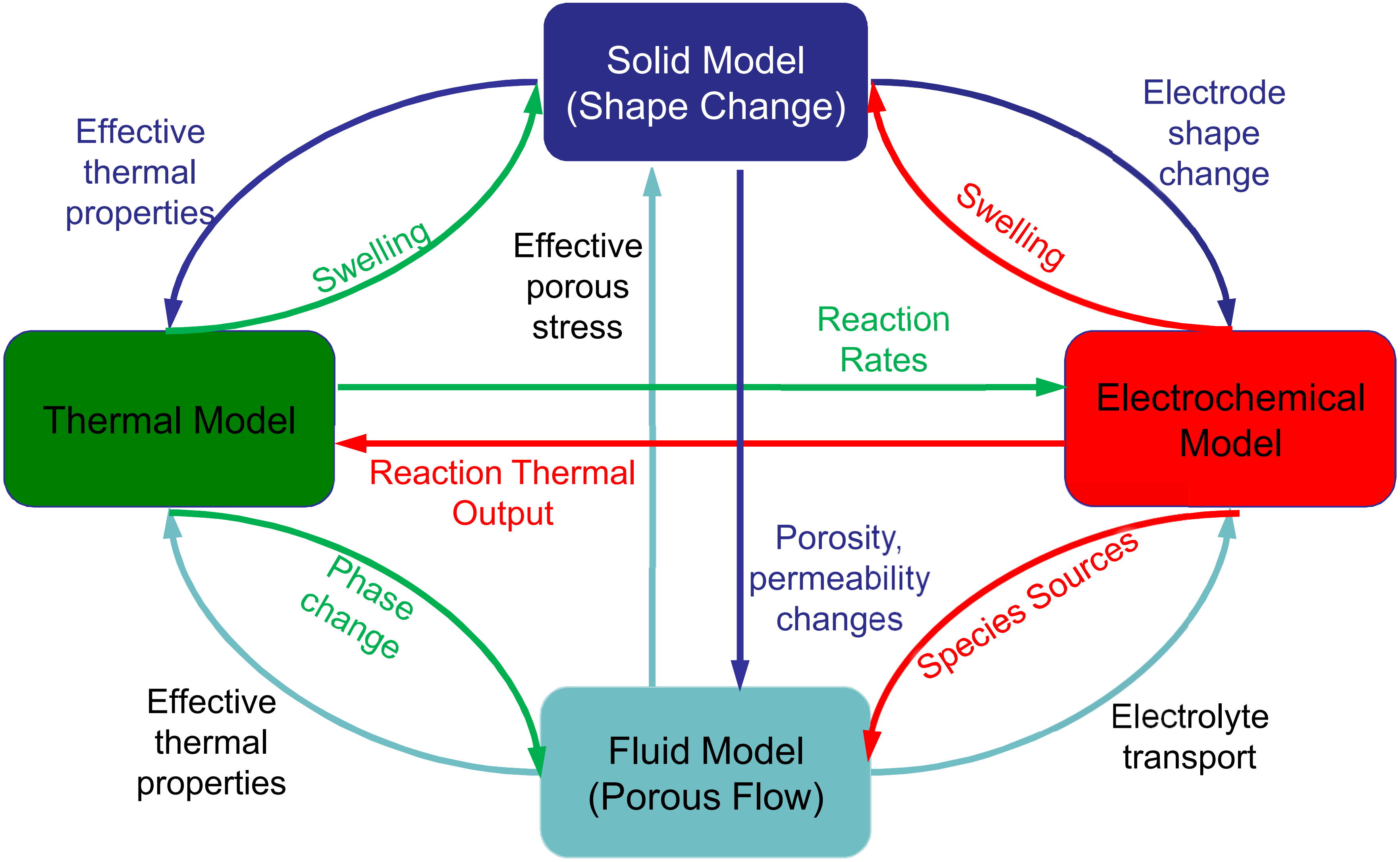

Physical models and couplings: Ideal

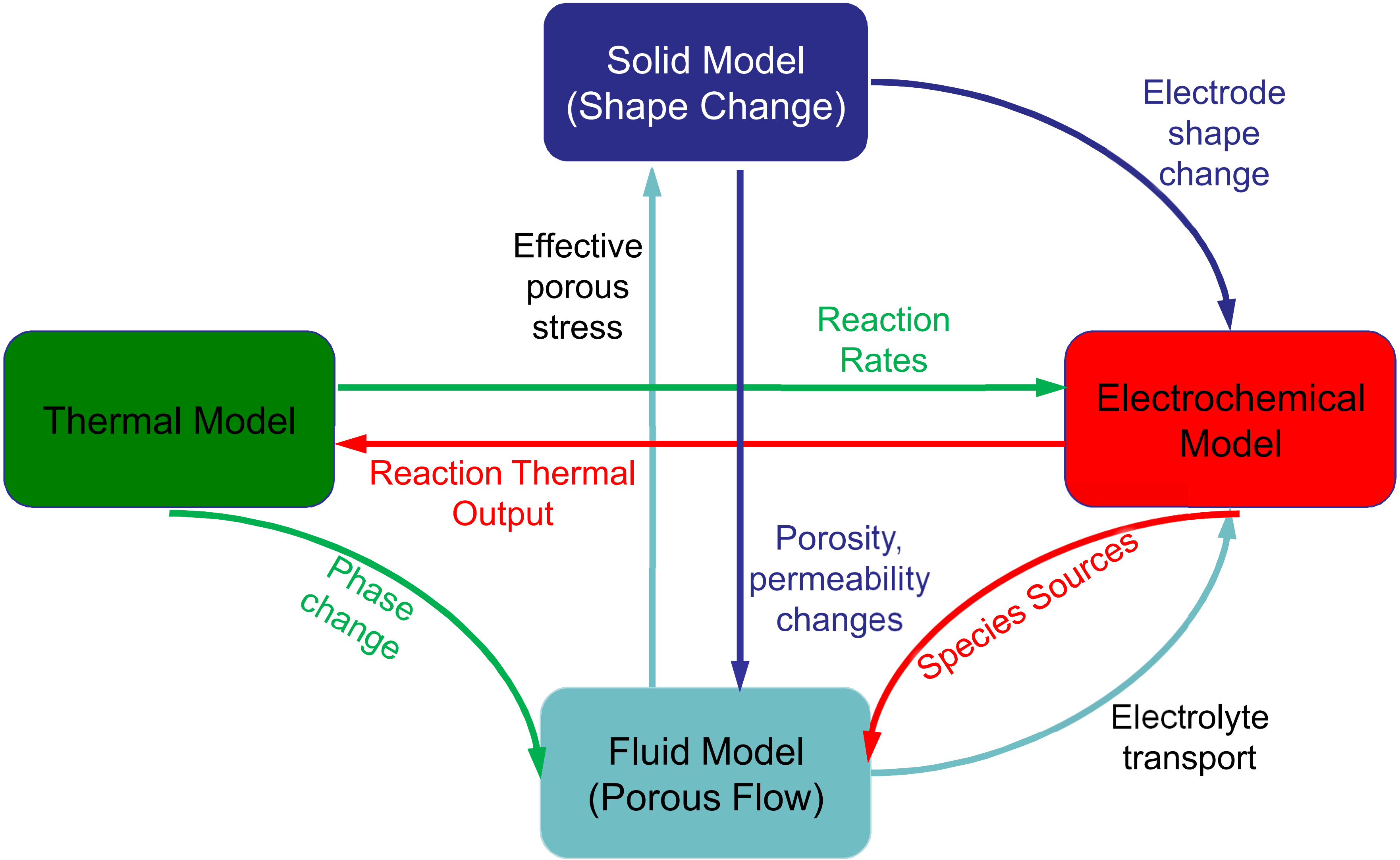

Models and demonstrations

- Thermo-poro-mechanical coupling
  - Thermal model
  - Mechanical deformation model
    - Thermo-mechanical demonstration
  - Porous flow model
    - Thermo-porous flow demonstration
  - Coupled thermo-poro-mechanical demonstration problem

- Thermo-electrochemical coupling
  - Electrochemical model
  - Demonstration problem

Models: Thermal

- Standard heat equation:

$$\frac{\partial T}{\partial t} = \alpha \nabla^2 T + Q$$

  - Source term *Q* applies to heat pellet, paper

- Level set tracking of burn fronts
  - Constant propagation speed
  - Heat released over a narrow region near burn-front position

- Presented at Power Sources 2012
  - Paper 30-2

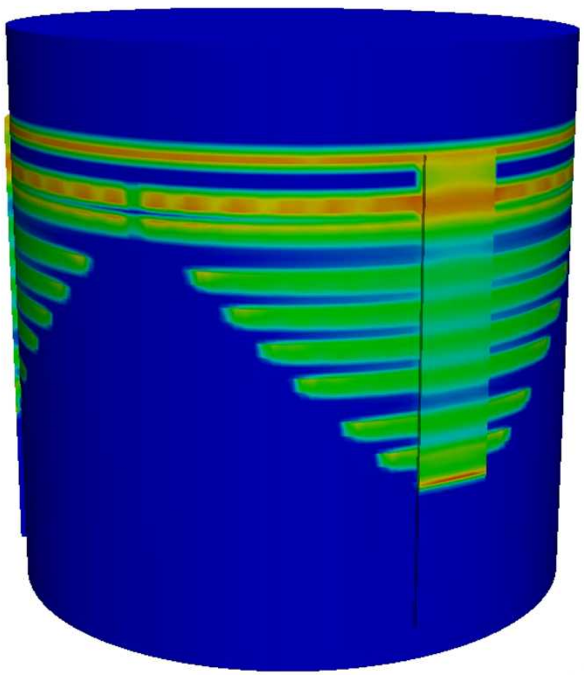

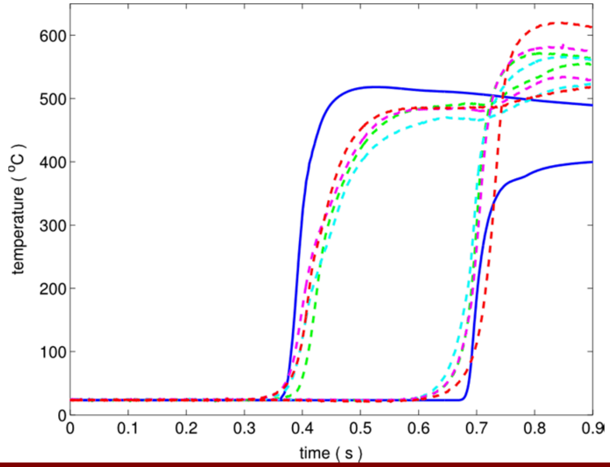

Model: Mechanical deformation

- Custom constitutive model
  - Capture the inelastic volumetric and isochoric deformation of the *MgO skeleton* before, during, and after activation
  - Isotropic, thermal-elastic-plasticity
  - **Plasticity governs activation deformation**
  - Kinematic split of deformations

$$\underline{F} = \underline{F}^e \underline{F}^p \underline{F}^T$$

  - Rule of mixtures for phase decomposition

$$\chi = \frac{T - (T - T_w/2)}{T_w}$$

  - Kirchoff stress: $\underline{\underline{\tau}} = \mu_x(T)\,\mathrm{dev}(\underline{b}^3) + \frac{\kappa_x(T)}{2}(J_e^2 - 1)\underline{\underline{\delta}}$

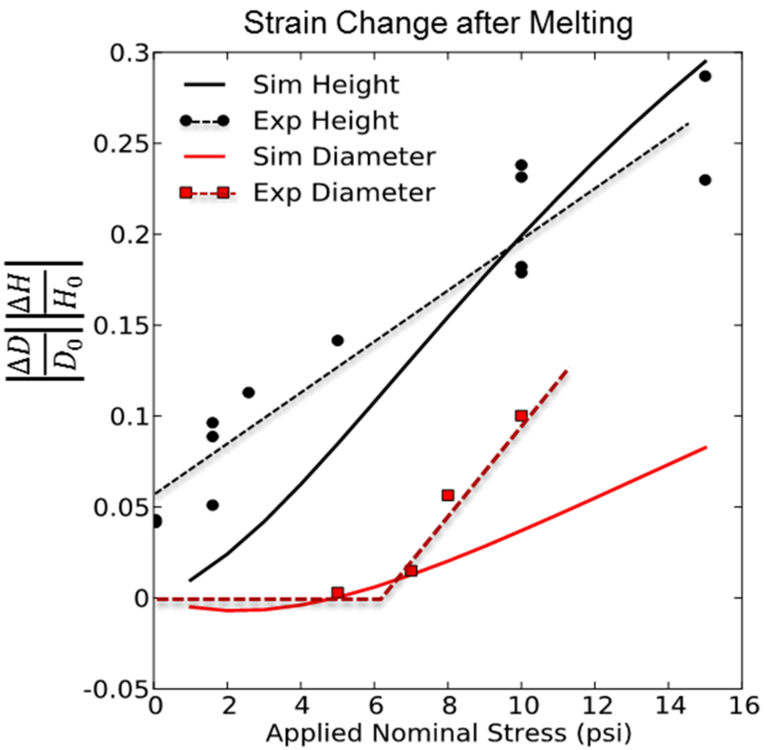

- Conservation of momentum: $\underline{\nabla} \cdot \underline{\sigma} = \underline{0}$

- Coupled to porous-flow through effective stress: $\underline{\sigma} = \underline{\hat{\sigma}} + p\underline{\delta}$

Demonstration: Themo-mechanical deformation

- As the separator heats to above the electrolyte melting temperature, the separator mechanically deforms in a process calibrated to experimental data.
- Current models capture the height change well, but not the diameter change
  - Related to the lack of effective stress in current implementation
  - Will be improved with thermo-poro-mechanical coupling

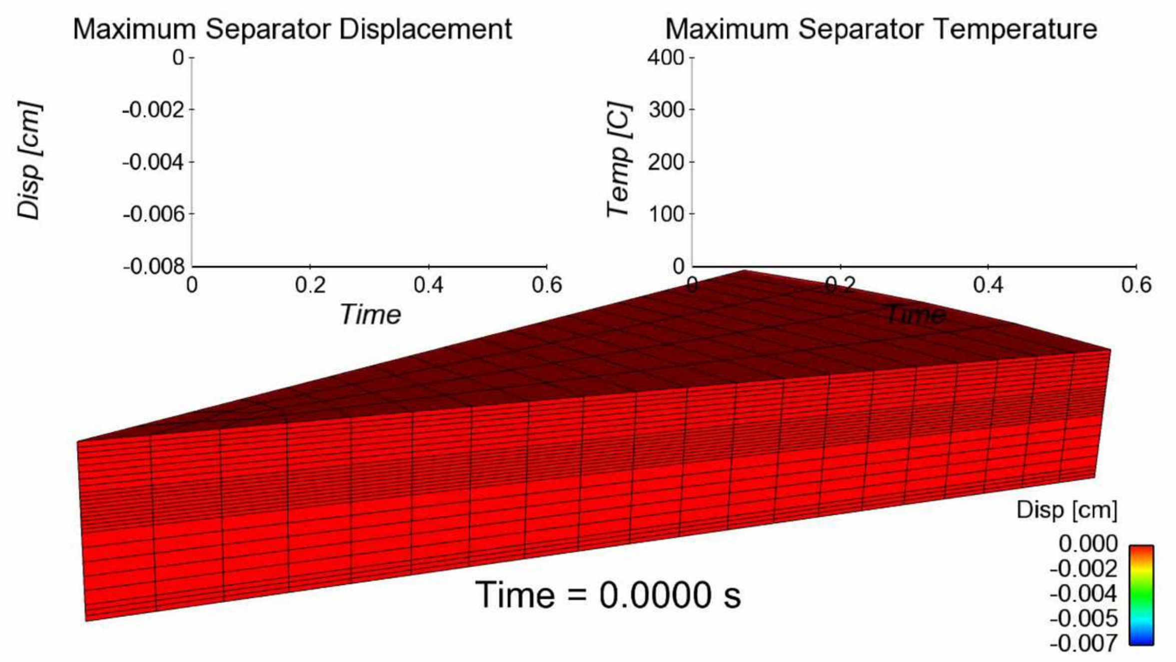

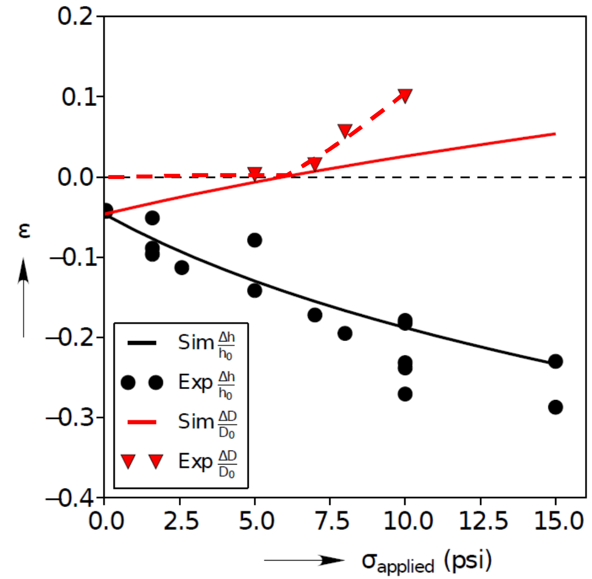

Models: Porous flow

- Electrolyte and gas form two immiscible phases upon melting

$$\frac{\partial(\rho_w \phi S_w)}{\partial t} = \underline{\nabla} \cdot \left(\rho_w \frac{k_{rw}}{\mu_w} \underline{\underline{K}} \cdot (\underline{\nabla} p_w - \rho_w \underline{g}) \right) + Q_w$$

$$\frac{\partial(\rho_n \phi S_n)}{\partial t} = \underline{\nabla} \cdot \left(\rho_n \frac{k_{rn}}{\mu_n} \underline{\underline{K}} \cdot (\underline{\nabla} p_n - \rho_n \underline{g}) \right) + Q_n$$

- Saturation and capillary pressure related to DOFs (wetting and non-wetting pressures) through model relations

$$S = S(p_c); \quad p_c = p_n - p_w$$

- Coupling to other physics important!
  - Required:

$$\phi = \phi(\underline{d}); \quad \mu_i = \mu_i(T)$$

  - Optional?:

$$S_i = S_i(p_c, \underline{d}); \quad \underline{\underline{K}} = \underline{\underline{K}}(\underline{d})$$

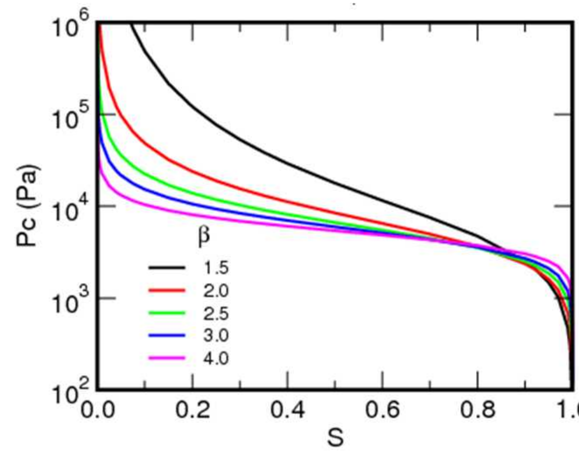

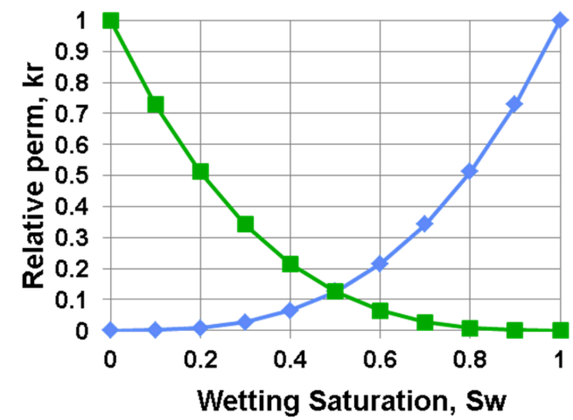

Capillary pressure (top) and relative permeability (bottom) depend on wetting phase saturation and electrode pore structure

Demonstration: Thermo-porous flow

- Two-pressure porous-flow formulation enables stable solution of flow from the separator to the cathode and anode.
- Flow is "frozen" before activation by an artificially high viscosity. As the electrolyte melts, the viscosity drops.

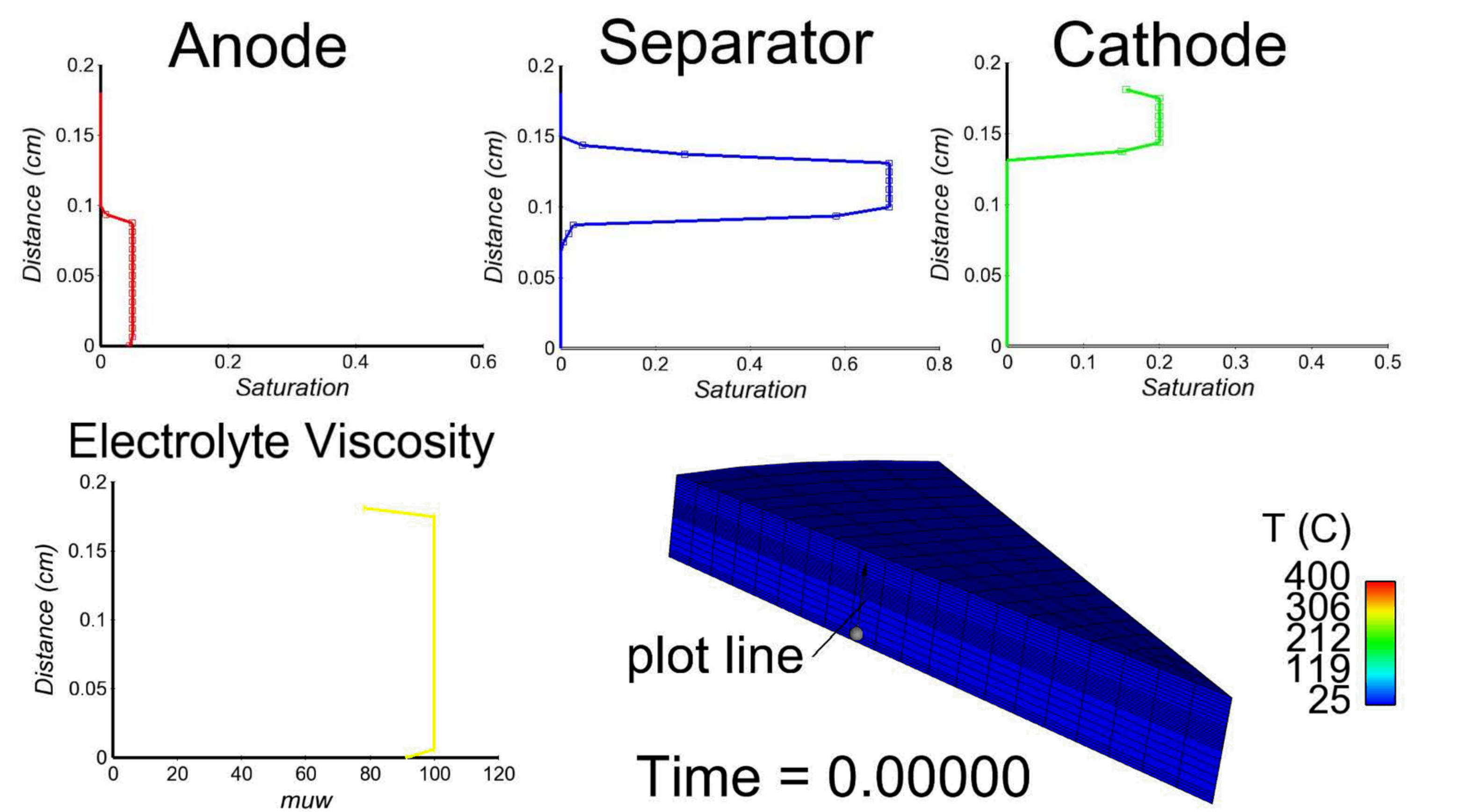

Demonstration: Thermo-poro-mechanical coupling

- Thermo-poro-mechanical single-cell simulation with full coupling:
  - Heat pellet burn
  - Two-phase porous flow upon activation
  - Separator deformation upon activation

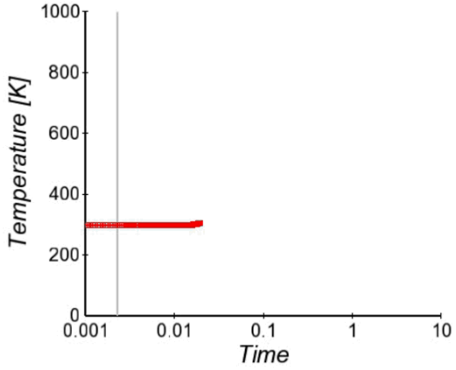

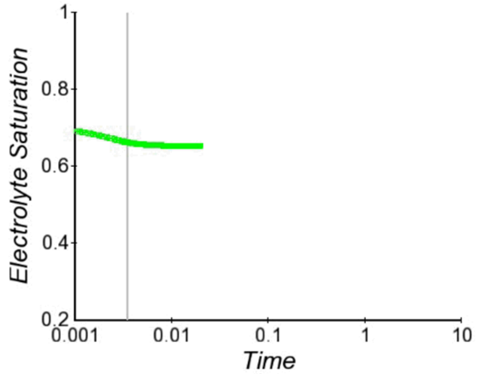

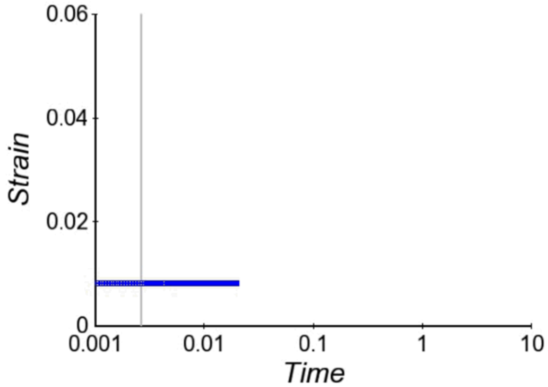

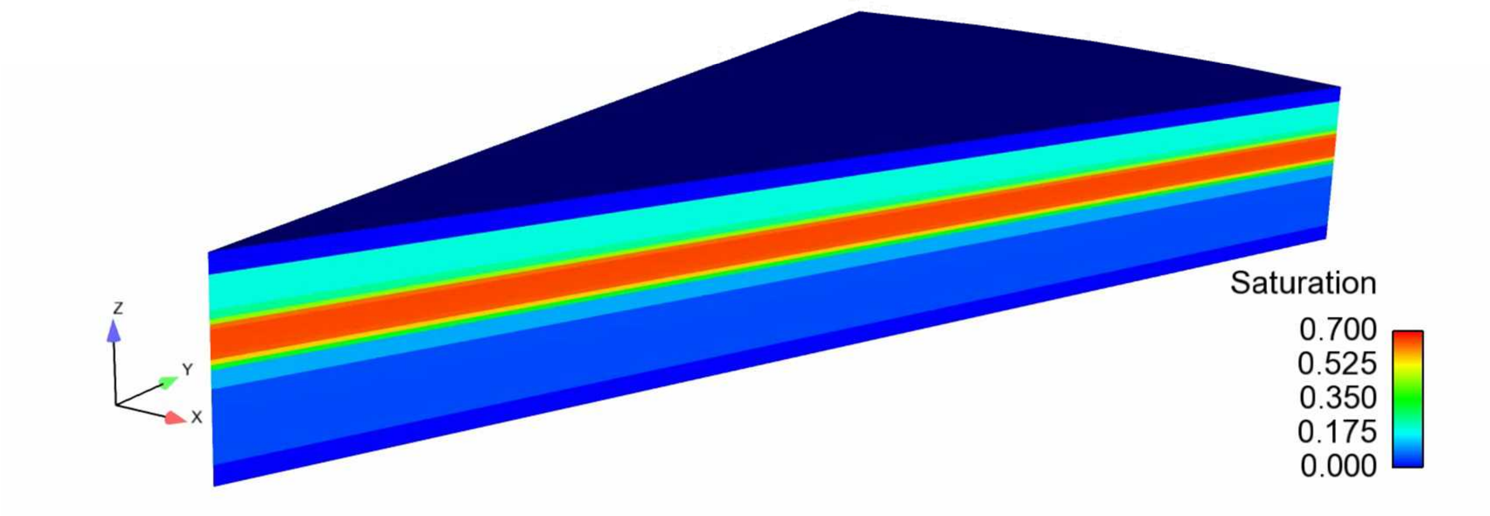

Models: Electrochemistry

- Reactions, especially for the cathode, are stoichiometrically complicated

$$\text{Cathode}: FeS_2 \leftrightarrows Li_3Fe_2S_4 \leftrightarrows Li_{2+x}Fe_{1+x}S_2 + Fe_{1-y}S \leftrightarrows Li_2FeS_2 \leftrightarrows Li_2S + Fe$$

$$\text{Anode}: Li_13Si_4 \leftrightarrows Li_7Si_4 \leftrightarrows 4Si$$

- Cantera's "Electrode Object" deploys multiple sub-grid models
  - Infinite capacity
  - Multi-plateau
  - Newman reaction extend
  - Finite capacity

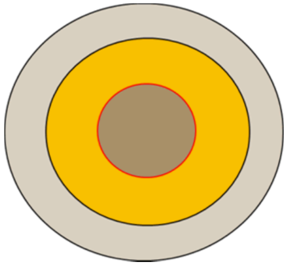

Shrinking Core Model

- Multiple plateaus can react simultaneously
- Diffusional losses with transport

- Primary electrochemical coupling is the temperature
  - Cantera's thermodynamics all temperature-dependent

- Future: Use deformed geometry to affect porosity in electrochemical calculations

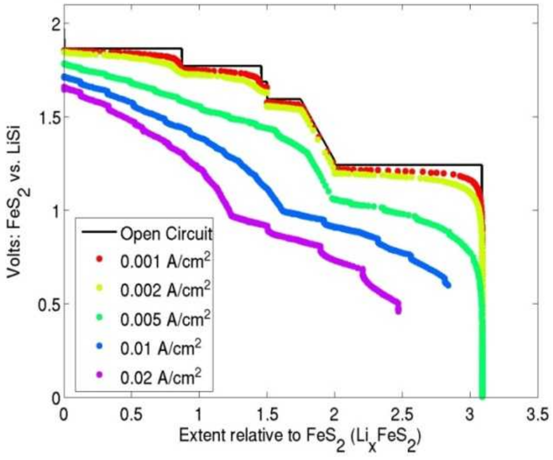

Demonstration: Thermo-electrochemical coupling

- Voltage responds to temperature and current

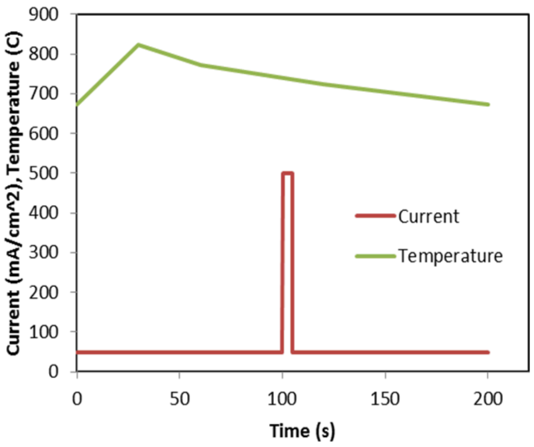

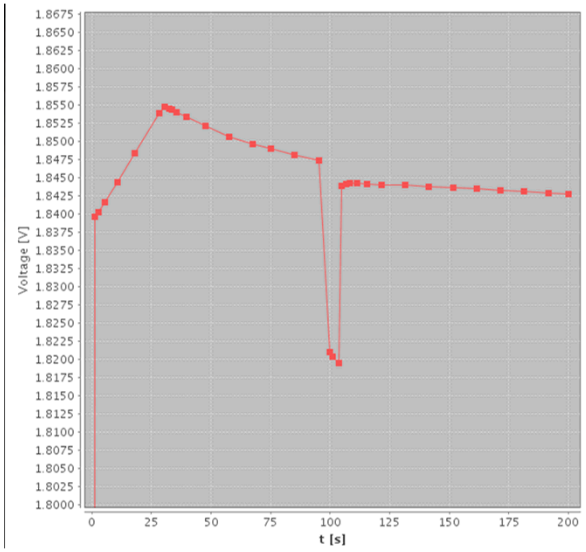

- Spatial temperature variations affect local potentials and current densities

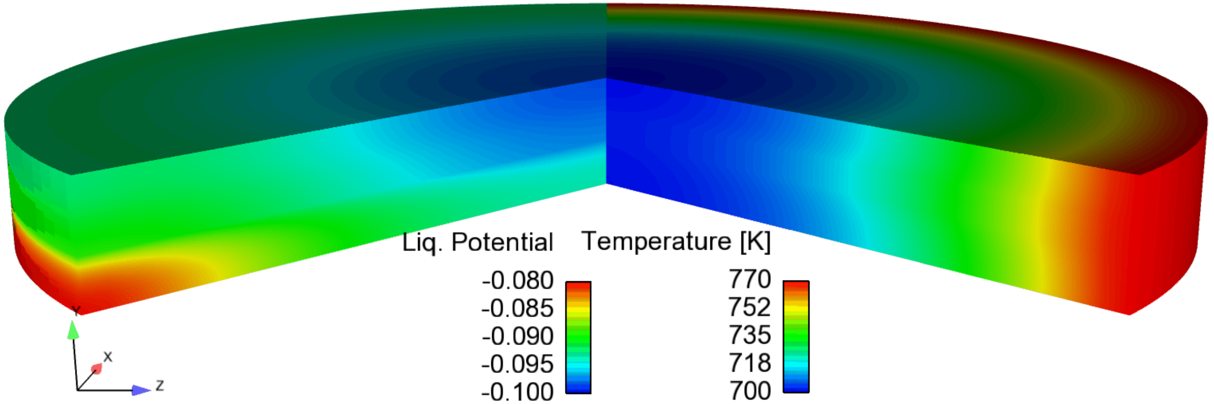

Summary

- “Intelligent” coupling of physics can provide significantly higher-fidelity models, with potentially only modest performance penalties.

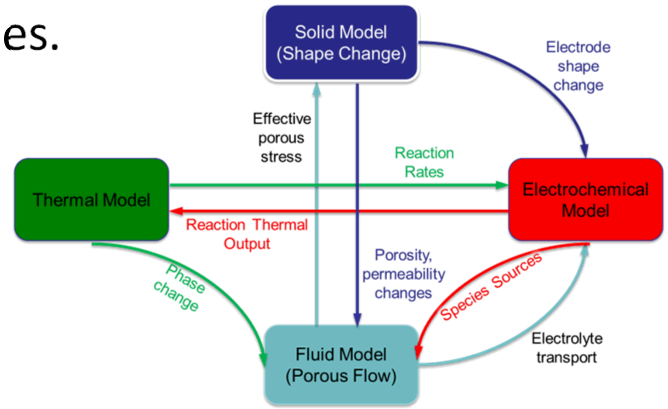

- Future investigation of additional couplings:
  - Material properties for all physics affected by:
    - Mechanical deformation (change in solid fraction)
    - Saturation (change in liquid fraction)
  - Eventually couple electrochemistry to the thermo-poro-mechanics

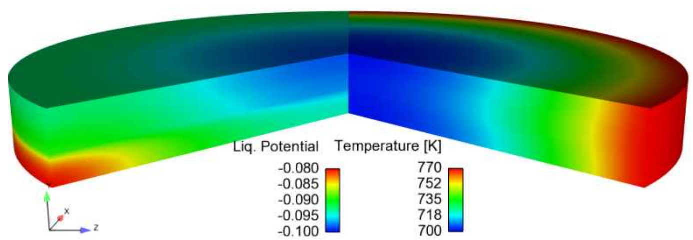

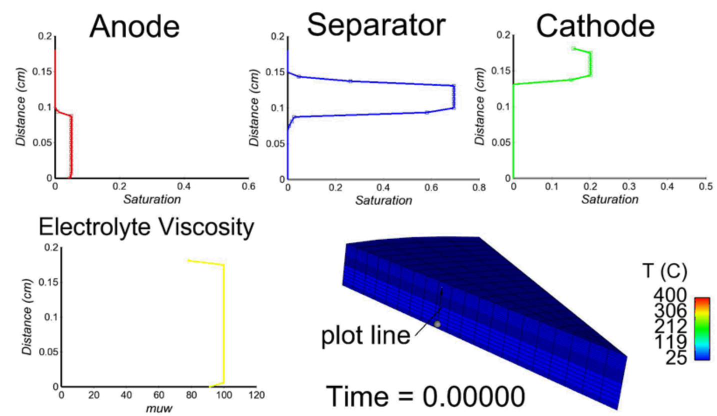

- Acknowledgements:
  - DoD/DoE Joint Munitions Program, TCG V
  - NNSA’s Advanced Simulation and Computing P&EM and WSEAT programs
  - Victor Brunini, Lindsay Erickson, Adrian Kopacz

BACKUP

Thermal-Mechanical Behavior of the Solid Skeleton

Free Energy Density

$$\rho_0\psi = \mu_x[T](\bar{I}_{1e} - 3) + \frac{\kappa_x[T]}{4}\left(J_e^2 - 1 - 2\log J_e\right)$$

Kirchoff Stress

$$\boldsymbol{\tau} = 2\rho_0 \boldsymbol{b}\frac{\partial\psi}{\partial\boldsymbol{b}} = \mu_x[T]\text{dev}[\boldsymbol{b}^e] + \frac{\kappa_x[T]}{2}\left(J_e^2 - 1\right)\mathbf{1}$$

Isochoric (Radial) Yield

$$\phi_\mu = \sqrt{J_2} - A_x\frac{I_1}{3} - B_x\left(\frac{I_1}{3}\right)^2 - Y_{ps\,x} - H_{\mu\,x}\epsilon_\mu^{m_x}$$

Plastic Flow Rules

$$\mathcal{L}\left[\boldsymbol{b}^e\right] = \boldsymbol{F}\dot{\boldsymbol{C}}^{p-1}\boldsymbol{F}^T = -2\left(\dot{\lambda}_{iso}\boldsymbol{n}_{iso} + \dot{\lambda}_{vol}\boldsymbol{n}_{vol}\right)\boldsymbol{b}^e$$

$$\boldsymbol{n}_{iso} = \frac{\text{dev}\boldsymbol{\tau}}{||\text{dev}\boldsymbol{\tau}||}, \qquad \boldsymbol{n}_{vol} = \frac{1}{3}\mathbf{1}$$

Kinematic Split of the Deformation Gradient: Thermal, Elastic, and Plastic Parts

$$\boldsymbol{F} = \boldsymbol{F}^e\boldsymbol{F}^p\boldsymbol{F}^\theta$$

Cold/Hot State Phase Decomposition

$$\begin{aligned}
&\text{if} && T < T_m - T_w/2, && \chi = 0,\\
&\text{elseif} && T > T_m + T_w/2, && \chi = 1,\\
&\text{else} && && \chi = \frac{T - (T - T_w/2)}{T_w},
\end{aligned}$$

Volumetric Yield

$$\phi_\kappa = \frac{I_1}{3} - Y_{P\,x} - H_{\kappa\,x}\epsilon_\kappa^{n_x}$$

Net Yield Surface is the Phase Volume Fraction Weighted Sum

$$\phi = (1-\chi)\left(\phi_\mu^C + \phi_\kappa^C\right) + \chi\left(\phi_\mu^H + \phi_\kappa^H\right)$$